On the wall boundary condition for the velocity in concentrated suspensions

C. Varsakelis[a,*], V. Gelbgras[b], M.V. Papalexandris[a]

[a] *Institute of Mechanics, Materials and Civil Engineering*
Univesité catholique de Louvain, B1348 Louvain-la-Neuve, Belgium
[b] *Independent Consultant, B1300 Wavre, Belgium*

Abstract

Continuum models for concentrated suspension have succeedded in reproducing most features of channel flows, except for volume-fraction profiles in the vicinity of the walls. It has been stipulated that this could be traced to the choice of the no-slip boundary condition for the velocity of the granular phase, which conflicts experiments indicating the existence of a slip layer. In fact, particle migration is inhibited in the absence of sufficient slip and, therefore, numerical simulations tend to overestimate the volume fraction. In this paper, we explore whether apparent slip and true slip boundary conditions can mitigate those discrepancies. Our study suggests that when adequate slip is prescribed at the wall, the numerical predictions can match the experimentally observed values near the walls. However, there is a complex correlation between required slip and the average concentration; this is in line recent experimental measurements of the near-wall slip in concentrated suspension

Keywords: granular suspensions, boundary conditions, concentrated suspensions, two-phase continuum models, wall slip

1. Introduction

Channel flows constitute a critical benchmark case for continuum models of non-Brownian suspensions. This is because, despite their conceptual

*Corresponding author
Email address: christos.varsakelis@gmail.com (C. Varsakelis)

simplicity, they exhibit typical characteristics of suspensions including the formation of a central plug zone [1], shear-induced particle migration [2, 3], and a fairly smooth particle concentration peak at the center of the channel [4, 5], all of which are non-trivial to reproduce numerically [6].

Recent studies have systematically been successful in reproducing the main features of the flows of interest [6–12]. However, a notable limitation of them was that they did not accurately capture the profile of the particle volume fraction in the vicinity of walls. Collectively, continuum models tend to overestimate the values of the volume fraction and cannot predict a layer of decreasing particle concentration with a minimum at the wall that has been documented through both experiments [3, 4, 13, 14] and particle-based simulations [14, 15]. To date, various attempts have been made to explain this discrepancy between experimental data and numerical predictions. These can be classified in three categories.

The first category consists of experiment-based explanations. According to them, measuring the volume fraction in the neighborhood of the wall is arduous and prone to high uncertainty. The difficulty of near-wall measurements is mentioned in both numerical studies [7, 16, 17] as well as experimental ones [2, 3, 10, 11, 13]. The argument then goes that, with such large error bounds, the near-wall layer of decreasing concentration might be fictitious. However, upon summarizing different experimental measurements, Yeo & Maxey [14] asserted that uncertainty is predominately due to the systematic overestimation of the volume fraction values. In turn, this implies that it is not the existence of a decreasing wall layer of particle concentration that is a matter of debate but its slope and exact values. Additional evidence in this direction is provided by the follow-up experimental study of Lyon & Leal [18]. Those authors carried out experiments with bi-disperse suspensions employing, on top of their previously used laser Doppler velocimetry method, a particle tracer concentration one, which is well adapted for near wall measurements. Now, some care needs to be exercised when extrapolating results from polydisperse suspensions to monodisperse ones, even only due to the Brazilian nut effect [19]. With this in mind, the results in [18] showcase the presence of a wall layer for the larger suspension particles.

Explanations of the second category orient towards limitations stemming from the continuum hypothesis. Owing to the presence of the particle diameter, suspensions exhibit a scale segregation. Consequently, one may argue that at scales comparable to or smaller than the particle diameter the validity of continuum models becomes questionable. Whilst ostensibly appealing,

this argumentation has to be juxtaposed with the theoretical foundations of continuum models. The basic hypothesis is whether a collection of particles can be described as a continuum fluid, endowed with its own unique properties. To test this hypothesis, one can rigorously start from the axiomatic foundations of continuum mechanics adapted for solid-fluid mixtures; see, for instance, [20, 21]. Accordingly, the volume fraction is formally derived as a field variable; more specifically, as the Radon-Nikodym derivative of the natural Lebesgue measures associated with the fluid and the solid phases, respectively. It then follows that the particle phase is no longer a collection of particles but a continuum, defined point-wise in analogy with a fluid. As pointed out by Koh et al. [2], disagreement with experiments due to particle-scale related effects should be traced to the inadequate accommodation of these effects into the continuum model and not to the continuum hypothesis itself. For example, this has been successfully mitigated for the case of the interphasial drag coefficient [22].

Explanations of the third category have attributed the problem to the choice of boundary conditions. Because the volume fraction is an internal variable, the prescription of physically justifiable boundary conditions is not straightforward. It was therefore hypothesized that the problem in hand could be rectified through the accommodation of different boundary conditions for the volume fraction. However, studies that have used Dirichlet conditions [23, 24], zero-particle flux conditions [6, 10, 11] and symmetry based conditions [7] have all yielded unsatisfactory results and this hypothesis can been put to rest. The focus has since turned on the boundary condition for the suspension velocity. Thus far, the vast majority of numerical studies have employed the no-slip boundary condition [7, 11, 12, 25–29]. However, there is conclusive experimental evidence corroborating the presence of a thin lubrication layer between the wall and the first layer of particles, where the shear rate is higher [30–33]. To this extent, in order to control slip, experimental campaigns oftentimes glue a layer of particles at the wall to increase the surface roughness at a scale similar to the particle diameter [34–36]. In turn, this renders the overall appropriateness of the no-slip boundary condition questionable and suggests the consideration of apparent slip boundary conditions as more physically relevant alternatives. In fact, the prescription of an apparent slip boundary condition as a remedy for the so-called volume fraction prediction gap was recently suggested by Li et al. [12].

The recommendation of Li et al. [12] has been already interrogated in [37], the difference being that the latter study, which actually predates that of [12],

has employed a mixture model whilst the former has opted for a two-phase one. Gavrilov & Shebelev [37] precisely utilized an apparent wall boundary condition for the suspension velocity but were unable to reproduce the wall layer of the volume fraction. In fact, upon further inspection, we can readily deduce that the numerical predictions [37] are only but slightly different to those obtained from no-slip conditions; e.g. [7]. One may then argue that the imposed slip was not large enough to onset particle migration towards the center and thus the formation of the lubrication layer adjusted to the walls. Evidence in favor of this argument stem from the fact that Gavrilov & Shebelev [37] employed verbatim the slip coefficient correlation proposed by [38]. While those authors mentioned that they did so to avoid a retrofitting of their predictions to experimental measurements, recent experimental efforts [33], however, have showed that the original correlation in [38] is not always sufficiently accurate.

In this paper, we extend the work of Gavrilov & Shebelev [37] in two directions. First, we examine whether the introduction of slip at the wall can alter the volume fraction profiles. To do so, we prescribe the two-phase model [39] with a true slip condition and then carry out a parametric analysis with respect to the slip coefficient value. It is shown that variations of the slip coefficient translate into qualitative differences in the volume fraction profile. Based on the results of this analysis, we then endow the same model with an apparent slip boundary condition that is, nevertheless, different from that in [37] to better fit with the two-phase framework that we have employed. For moderate to high concentrations, we are then able to reproduce the near-wall layers of decreasing particle concentration. For higher concentrations, however, this is not the case. Collectively, our predictions corroborate the experimental analysis in [33], pointing towards a complex correlation between the necessary slip and the average concentration.

2. Governing equations

Our numerical study of channel flows is based on the two-phase thermo-mechanical model for concentrated suspensions developed in [7]. The channel width is sufficiently small so that the suspensions can be assumed to be neutrally buoyant. Then, for the flows of interest, the model reduces to a system of nonlinear ordinary differential equations. Herein, we simply

reproduce the final equations which in dimensionless form read [7],

$$\frac{1}{Re}\frac{\mathrm{d}}{\mathrm{d}y}\left(\phi_f\frac{\mathrm{d}u_f(y)}{\mathrm{d}y}\right) = \delta(u_f-u_s)-F\phi_f\,, \tag{1}$$

$$\frac{1}{Re}\frac{\mathrm{d}}{\mathrm{d}y}\left(\mu_s\phi_s\frac{\mathrm{d}u_s(y)}{\mathrm{d}y}\right) = -\delta(u_f-u_s)-F\phi_s\,, \tag{2}$$

$$\frac{1}{Re}\frac{\mathrm{d}}{\mathrm{d}y}\left(\mu_n\phi_s\left|\frac{\mathrm{d}u_s(y)}{\mathrm{d}y}\right|\right) = -\frac{\mathrm{d}}{\mathrm{d}y}\left(\gamma_s\left(\frac{\mathrm{d}\phi_s}{\mathrm{d}y}\right)^2\right)-\frac{\mathrm{d}}{\mathrm{d}y}(p_s\phi_s)\,, \tag{3}$$

$$p_s-\beta_s+\frac{\mathrm{d}}{\mathrm{d}y}\left(\gamma_s\frac{\mathrm{d}}{\mathrm{d}y}\phi_s\right) = 0\,, \tag{4}$$

$$\phi_s+\phi_f = 1\,. \tag{5}$$

Equations (1) and (2) describe the balance of (linear) momentum in the streamwise direction for the fluid and granular phase, respectively. Equation (3) is the momentum balance law for the granular phase in the normal direction. Also, the compaction equation (4) governs the evolution of the volume fraction of the granular phase [40] and (5) is the saturation relation.

In the above equations, the subscripts "f" and "s" designate the fluid and particle (solid) phase, respectively. Accordingly, u_i, p_i, ϕ_i, and μ_i denote the velocity, pressure, volume fraction and shear viscosity of the phase $i = s, f$. Further, μ_n the normal viscosity of the granular phase, while F is the applied pressure gradient that maintains the flow and δ is the interphasial drag coefficient. The Reynolds number Re is defined with respect to the fluid density, the centerline velocity of the equivalent single-phase fluid flow, the channel half-width l_{ref} and the shear viscosity of the fluid μ_f; see [7] for more details. The coefficient β_s is the intergranular stress coefficient and represents resistance of grains under compaction; finally γ_s is a Korteweg-type coefficient [40, 41].

To close the governing equations, we use the same correlations used in [7]. For the drag law, an extension of the Hill-Koch-Ladd drag correlation (valid for a wide range of volume fractions and Reynolds numbers) is used [22]. The exact formula is too cumbersome to reproduce herein.

For the viscosity coefficients μ_s and μ_n we adopt the formulae proposed

in [42],

$$\mu_s \;=\; \frac{2.5}{\phi_{jam}-\phi_s} + 0.1\frac{\phi_s}{(\phi_{jam}-\phi_s)^2}\,, \tag{6}$$

$$\mu_n \;=\; 0.75\frac{\phi_s}{(\phi_{jam}-\phi_s)^2}\,, \tag{7}$$

with $\phi_{jam} = 0.6$ is the jamming transition volume fraction. Both μ_s and μ_n have been non-dimensionalized with respect to μ_f.

For the intergranular stress β_s we employ a slightly modified version of the correlation derived in [43] which reads,

$$\beta_s \;=\; -\beta_0\,\log(\phi_{jam}-\phi_s)\,, \tag{8}$$

with $\beta_0 = 1.04\times 10^3$. Finally, for γ_s, we adopt the following power law discussed in [7],

$$\gamma_s \;=\; -\gamma_0\,\phi_s^6\,, \tag{9}$$

with $\gamma_0 = 5.2\times 10^4$; this value has been obtained through fitting against experimental measurements [39].

With regard to boundary conditions for the volume fraction, we follow [7] and impose the following integral condition supplemented with a symmetry at the boundary that both stem from the properties of the channel flow,

$$\int_{-1}^{1}\phi_s\,\mathrm{d}y \;=\; 2\phi_{av}\,, \quad \text{and} \quad \phi_s(-1) \;=\; \phi_s(1)\,,$$

where ϕ_{av} is the average volume fraction of the flow. This choice allows for non-zero volume fraction gradients, in the direction normal to the wall.

The fluid phase is assumed to be Newtonian and, therefore we prescribe the no-slip boundary condition for its velocity. The boundary conditions for the granular velocity are discussed in the beginning of the corresponding results section.

3. Numerical results

A recent set of experimental measurements for the flows of interest was published in [4, 5]; in the original publications, the reported volume fraction values were truncated to the 80% of the channel and the full profiles were

communicated in [14]. We have opted to reproduce these experiments and, accordingly, we consider the channel flow of glycerin and water (ρ_f=1200 kg/m^3, μ_f=0.04 Pa s) with monodisperse silica solid particles (ρ_s=2100 kg/m^3, $D = 1\,\mu m$). The channel has width equal to 40μm and the Reynolds number is approximately $Re = 1.2 \times 10^{-4}$.

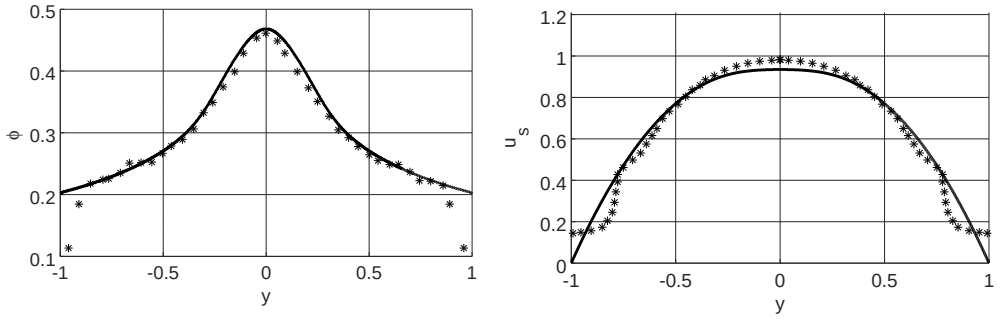
For the sake of completeness, in Figures 1a-1b we have plotted the predicted volume fraction and particle velocity profiles for the no-slip case, for average volume fractions $\phi_{av} = 0.298$ and $\phi_{av} = 0.411$. In the same figures we have plotted the experimentally measured volume fraction profile of [14] and the associated simulated granular velocity profile that the authors of [14] obtained by the Forced-Coupling-Method (FCM). For the volume fraction, one readily confirms the deviation of numerical predictions from the experimental measurements in the vicinity of the wall. In the remainder of the channel, good agreement is observed. Comparison of the velocity profiles follows a similar pattern, with differences being more pronounced in the neighborhood of the walls. According to the FCM profiles, a rapid drop in velocity occurs at approximately 1/4 of the distance between the wall and middle which is then followed by an (almost) plug zone. The authors of [14] attribute this characteristic to the due to the particle–wall lubrication interaction stemming from the FCM method. However, such a feature is absent from experimental measurements [3, 4].

3.1. True slip

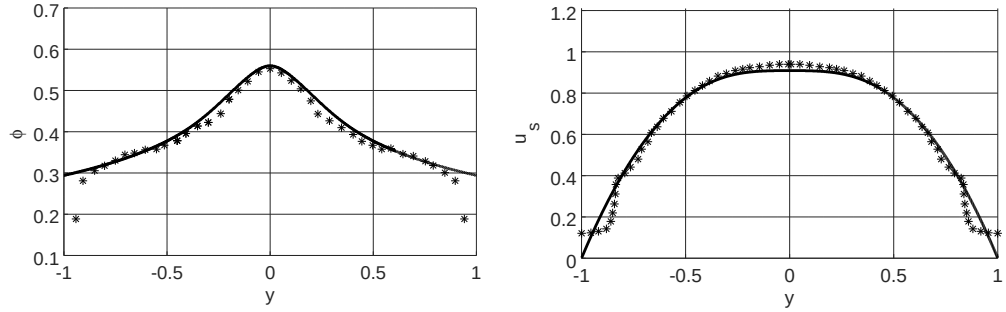
True slip is more likely to be present in single-phase viscous liquids such as polymer melts than in concentrated suspensions [44]. However, it constitutes the simplest and more controlled way for examining the effect of slip on the volume fraction profiles in a numerically straightforward manner. For the true slip boundary condition, one sets the value of the granular velocity at the wall proportional to a reference velocity. For channel flows, this is typically assumed to be the maximum velocity, so that we have,

$$u_s \;=\; A_{\text{slip}} u_{\max} \tag{10}$$

where $0 \leq A_{\text{slip}} \leq 1$ is an (experimentally determined) slip coefficient and $u_{\max}$ is the maximum velocity, which for the flow of interest lays at the center of the channel. We have carried out a parametric study with respect to A_{slip} for $A_{\text{slip}} \in [0, 0.3]$ for both $\phi_{av} = 0.298$ and $\phi_{av} = 0.411$. Figures 2a-2c depict the predicted volume fraction and granular velocity profiles, for $\phi_a v = 0.298$



(a) $\phi_{av} = 0.298$



(b) $\phi_{av} = 0.411$

Figure 1: No-slip condition: numerical predictions of the volume fraction and granular velocity profiles for two different average volume fractions ϕ_{av}. Top: $\phi_{av} = 0.298$; bottom: $\phi_{av} = 0.411$. $(-)$ numerical results; $(**)$ experimental data (volume fraction) and FCM-based predictions (granular velocity) [14].

and for $A_{\text{slip}} = 0.1, 0.15, 0.2$. As in the no-slip case, we have also plotted the experimental measurements for the volume fraction and the simulated granular velocity profiles of [14].

We first observe that, when the applied slip is low, the particle concentration follows a trend opposite to what is suggested by experiments and attains a local maximum in the wall. However, as A_{slip} increases, a steep layer of decreasing particle concentration is formed adjacent to the walls. The predicted profiles can, qualitatively, reproduce the experimental profiles, as the particle concentration approaches zero at the wall. The thickness of the decreasing layer, however, is shorter than the one suggested by experiments.

We also note the formation of local high-concentration zone next to the wall. The presence of non-monotonically decreasing profiles in the particle concentration (in the half channel) implies that particles are organized into distinct layers. Now, such particle layers have been reported in the numerical simulations of [14] (for planar flows) and the experimental measurements of [13, 45] (for pipe flows). Hampton et al. [13] attribute the formation of such layers to the restraining motion of the particles owing to the wall. While translation of this explanation to planar flows appears consistent, one still needs to confront the absence of experimental evidence. Yeo & Maxey [14] attempt to do so by comparing the experimental (and analytical) techniques of [3] and [13]. By so doing, they argue not that there might be some measurement error but also some statistical bias involved in computing the local volume fraction.

A third conclusion is that the effect of the slip on the particle concentration is local. Indeed, in the main body of the channel the profile remains unaltered and thus the overall agreement with experiments remains consistent. On the other hand, the velocity profile is globally shifted upwards. For the case $A_{\text{slip}} = 0.2$ we already note a noticeable global deviation from the experimental measurements. Moreover, our predictions show that the global minimum of the granular velocity is no longer at the wall, as expected, but rather in the interior of the channel (still close to the wall). Consequently, the predicted granular velocity has a local U-shape which, in turn, suggests that such true slip values are most likely nonphysically high. Comparison with the experimental values asserts that the most physically meaningful value for slip is in the vicinity of $A_{\text{slip}} = 0.15$.

The corresponding results for $\phi_{av} = 0.411$ case are plotted in 3a-3c. The effect that the the magnitude of A_{slip} has on the shape of particle concentration, especially near the walls, is similar to the $\phi_{av} = 0.298$ case. Upon

inspecting both cases, we deduce that, as the average concentration increases, so does that the magnitude of the slip required to reproduce the near-wall decreasing concentration layer. Still, $A_{\text{slip}} = 0.2$ is not sufficiently high to reproduce the near-wall particle layer.

At the some time, the effect of the slip remains local for the particle concentration and global for the granular velocity. In fact, the granular velocity fields depict the same trend as with the $\phi_{av} = 0.298$ cases. That is as A_{slip} increases, the overall field is shifted upwards. However, in contrast to the $\phi_{av} = 0.298$ case, this upward shift becomes more pronounced even at $A_{\text{slip}} = 0.15$, which again appears to be the most physically relevant value. Moreover, for $A_{\text{slip}} = 0.2$ we again observe the non-physical manifestation of the local U-shape in the proximity of the wall.

Overall, the true slip analysis indicates that for moderate concentrations ($\phi_{av} = 0.298$) introducing a reasonable amount of slip ($A_{\text{slip}} = 0.15$) suffices to qualitatively capture the near-wall decreasing layer of volume fraction. For higher concentrations, ($\phi_{av} = 0.411$), by extrapolating upon our results, it appears that the slip required to achieve the same results is much higher than what experiments dictate.

3.2. Apparent wall slip

Our next step is to prescribe an appropriate apparent slip condition to the granular velocity. For two-phase models, doing so is slightly more involved than in single fluid models, where only one velocity field is accounted for. Still, even for single fluid models, the starting point is a matter of debate. Defining the suspension velocity, u_{susp}, by

$$u_{\text{susp}} = \frac{\rho_s \phi_s u_s + \rho_f \phi_f u_f}{\rho_s \phi_s u_s + \rho_f \phi_f} = \phi_s u_s + \phi_f u_f \,, \tag{11}$$

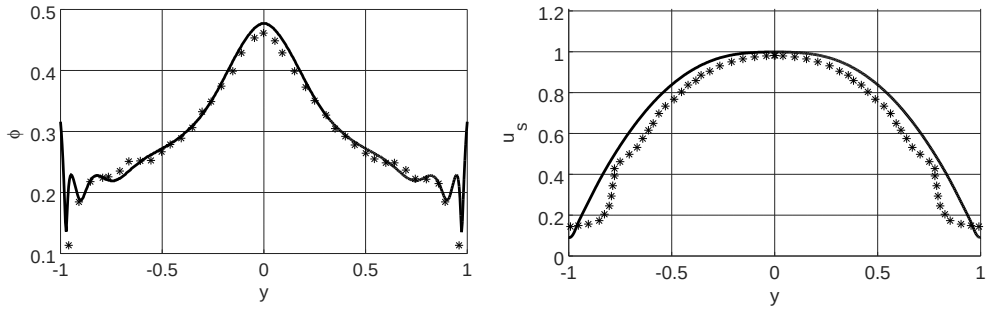
there are then two options, provided by [37] and [46], respectively. These options, when adjusted for the flow of interest, assume the following form,

$$\beta_w \delta_{\text{slip}} \tau_w \;=\; \mu_f u_{\text{susp}} = \mu_f \phi_s u_s \,, \tag{12}$$

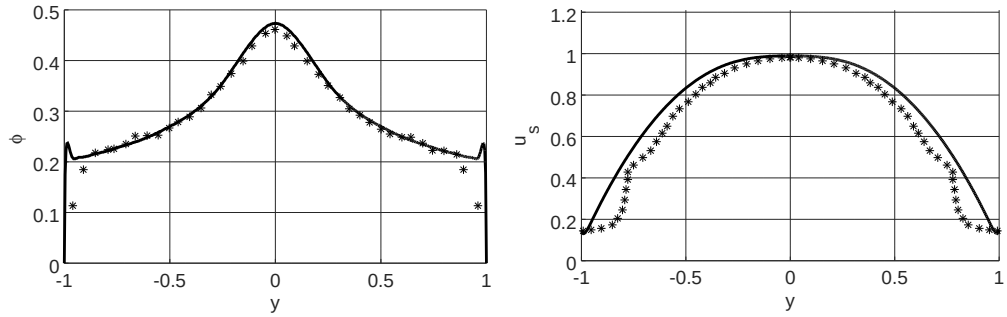
and

$$\beta_w \delta_{\text{slip}} \tau_w \;=\; \mu_f (u_s - u_f) = \mu_f u_s \,. \tag{13}$$

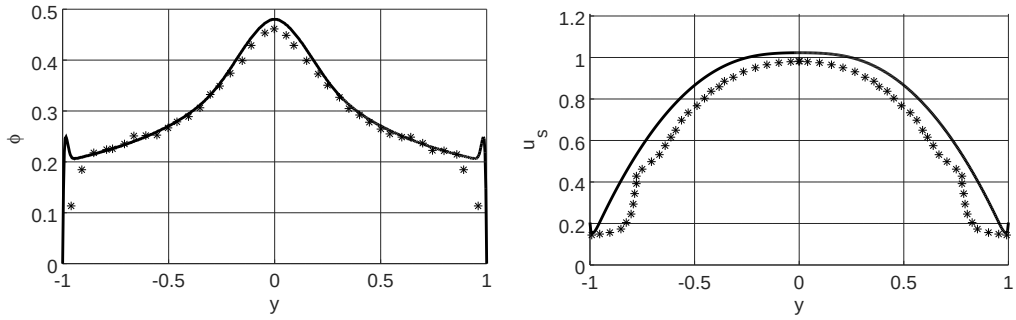
Here, β_w is the slip coefficient, δ_{slip} is the thickness of the slip layer, and τ_w is the traction. The above quantities are all evaluated at the wall. It then



(a) $A = 0.1$

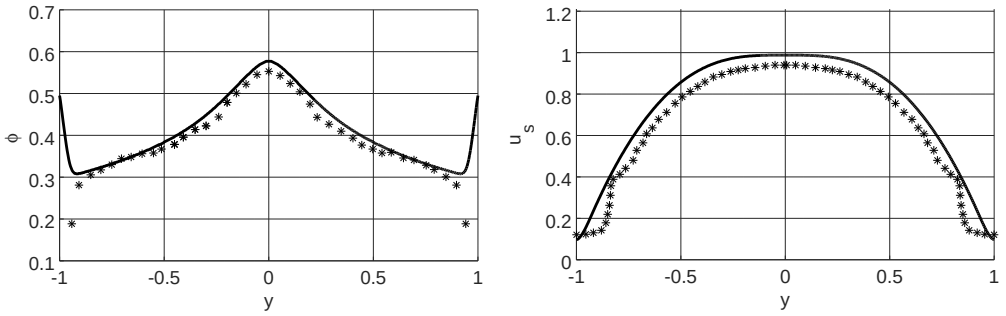


(b) $A = 0.15$

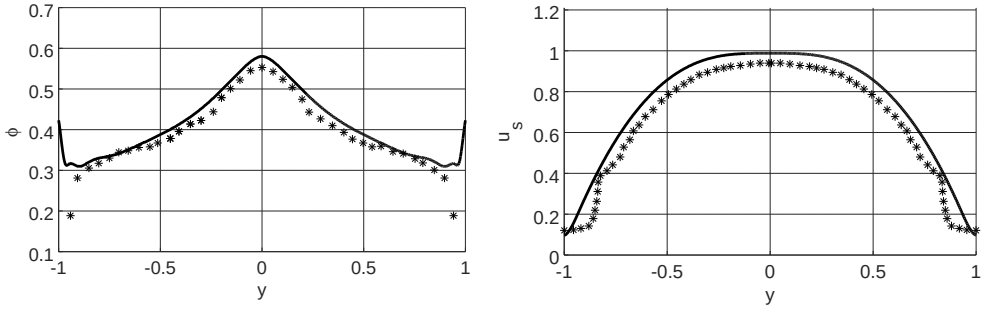


(c) $A = 0.2$

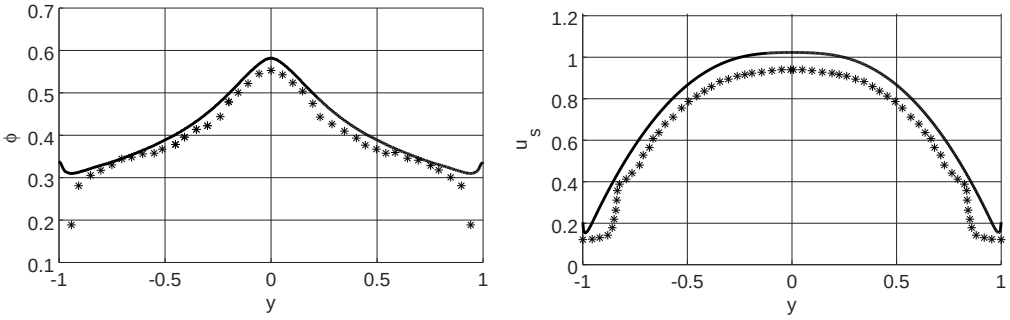
Figure 2: True slip condition: numerical predictions of the volume fraction and granular velocity profiles, for different slip coefficients A_{slip} and for $\phi_{av} = 0.298$. $(-)$ numerical results; $(**)$ experimental data (volume fraction) and FCM granular velocity simulations [14].



(a) $A = 0.1$



(b) $A = 0.15$



(c) $A = 0.2$

Figure 3: True slip condition: numerical predictions of the volume fraction and granular velocity profiles, for different slip coefficients A_{slip} and for $\phi_{av} = 0.411$. $(-)$ numerical results; $(**)$ experimental data (volume fraction) and FCM granular velocity simulations [14].

follows that, since the fluid is assumed to be a Newtonian one, $u_f = 0$. The main difference between (12) and (13) is the use of the suspension velocity in the first case instead of the granular velocity u_s in the second case as the variable that undergoes slip. Since the fluid velocity is assumed to vanish at solid boundaries, this difference amounts to using the "partial" velocity $\phi_s u_s$ in (12) instead of u_s in (13). Herein we opt for (13).

In the context of two-phase models, the overall traction is the sum of the contribution from each phase. Accordingly, its expression is obtained by combining the stress tensors of the particulate and fluid phases and then projecting onto the wall, which reads,

$$\tau_w \;=\; \mu_s \phi_s \frac{\mathrm{d}u_s}{\mathrm{d}y} + \mu_f \phi_f \frac{\mathrm{d}u_f}{\mathrm{d}y} \,. \tag{14}$$

As regards δ_{slip}, we employ the correlation provided in [38],

$$\delta_{slip} \;=\; D \left(1 - \frac{\phi_s}{\phi_j} \right) .$$

Finally, one may set $\beta_w = 1$ as a first guess, which is also the value typically used for suspension models. More specifically, fixing β_w to unity stems directly from [38], wherein β_w was found to be roughly equal to unity. Yet, as we mentioned above, more recent experimental studies have cast doubt on the robustness of this result, allowing for a variation at the order of a decade [33].

By combining the above relations, we derive the final expression for the apparent slip boundary condition for the particle phase,

$$u_s \;=\; \beta_w D \left(1 - \frac{\phi_s}{\phi_j} \right) \left(\frac{\mu_s}{\mu_f} \phi_s \frac{\mathrm{d}u_s}{\mathrm{d}y} + \phi_f \frac{\mathrm{d}u_f}{\mathrm{d}y} \right) . \tag{15}$$

If we compare the true slip with the apparent slip boundary conditions we find a major difference. True slip is Dirichlet boundary condition and, as such, is local in nature. By contrast, the apparent slip boundary is a Robin-type boundary condition and thus weakly non-local. Non-locality enters equation (15) through the incorporation of the granular velocity gradient at the wall (granular shear rate).

Figures 4a depict the numerical predictions for the volume fraction and the granular velocity for $\phi_{av} = 0.298$ against the experimental measurements for the volume fraction and the simulated granular velocity profiles of [14].

In direct analogy to the true slip case, the incorporation of apparent slip has also resulted in the reproduction of the near-wall layer of decreasing particle concentration. Moreover, the effect on the particle concentration remains local whilst for the particle velocity is global. However, we also infer that the induced slip is too high. Indeed, similarly to the $A_{\text{slip}} = 0.2$ case, we observe the appearance of the local U-shape in the vicinity of the wall. On top of that, we see that the discrepancy between predicted and measured values for the granular velocity is more pronounced; benchmarking is performed with respect to the no-slip results illustrated in figure 1a.

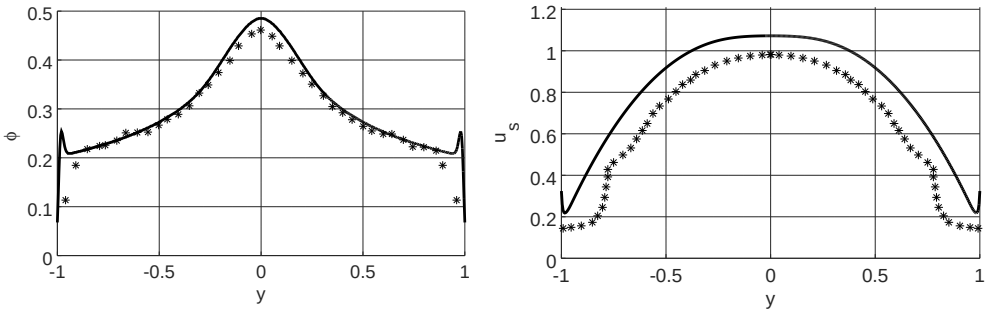
For the case of higher volume fraction, $\phi_{av} = 0.411$, our numerical simulations show that the prescribed slip is insufficient to reproduce the sought-after volume fraction behavior; see Figures 4b. We can map this result to the true slip case of $A_{\text{slip}} = 0.1$. This is also supported by looking at the granular velocity profiles, also plotted in Figure 4b. There is a slight, by clear, underestimation of the values at the boundary. Further, when juxtaposed to the no-slip case reported in figure 1b, the overall agreement with the FCM simulations of [14] has deteriorated. Still, the increase in the overall error is less than the $\phi_{av} = 0.411$ case.

Collectively, numerical predictions based on the apparent slip boundary condition follow the same trend as corresponding true-slip ones. That is, for moderately dense suspensions, it is possible to recover the wall-layer of decreasing particle concentration. For higher concentrations, however, this is not the case. On top of that, the introduction of the apparent slip boundary condition has increased the error in the granular velocity predictions.

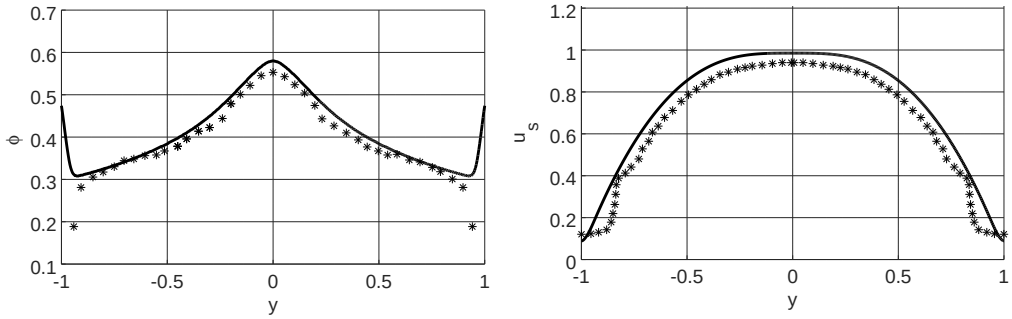
The overall picture, drawn from both numerical predictions and experimental measurements, is that the correlation between the average concentration, the magnitude of the slip coefficient and the wall granular shear rate is quite complex. Importantly, given (i) the success of our predictions in reproducing the flow features in the main body of the channel and (ii) the partial success in reproducing the wall layer (for moderate concentrations), we can conclude that the existing formulas for apparent slip are not sufficiently accurate. As mentioned above, this is in line with the experimental measurements [33] that suggest the revision of the original formulas in [38].

4. Discussion and conclusion

The present paper has examined whether a two-phase model, endowed with apparent slip and true slip boundary conditions can reproduce the near



(a) $\phi_{av} = 0.298$



(b) $\phi_{av} = 0.411$

Figure 4: Apparent slip: numerical predictions of the volume fraction and granular velocity for two different average volume fractions ϕ_{av}. Top: $\phi_{av} = 0.298$; Bottom: $\phi_{av} = 0.411$. $(-)$ numerical results; $(**)$ experimental data (volume fraction) and FCM granular velocity simulations [14].

wall layer of decreasing particle concentration in channel flows. It has been shown that for moderate concentrations, an appropriate choice of slip allows for the reproduction of the qualitative aspects of experimental measurements but this is not the case for higher concentrations. Collectively, our numerical simulations assert that the correlation between the required slip and the average concentration is more complex than the classical formulas for slip boundary conditions of [38] suggest. This corollary is in line with the experimental study [33] the results of which question the robustness of the extant empirical correlations.

An open question for future endeavors is the revision of the original correlation of [38] so as its accuracy and robustness are increased. One way forward could stem from the study of dry granular flows, where the prescription of accurate boundary conditions for the granular velocity and the volume fraction has also been the topic of detailed investigation, [47–49]. A common methodology therein has been based on carrying out particle simulations and thus directly inferring on the slip velocity [50, 51]. In principle, this analysis could be replicated for suspension flows as well, as Discrete Element Methods for suspensions are already available in the literature, [52, 53]. An alternative approach that has also been explored in dry granular flows is that of theoretical analyses [54, 55]. Extension to suspensions, however, is cumbersome owing largely to the coupling between the two phases through momentum exchanges. This coupling cannot be ignored even if we focus on the frictional motion of a particle on a surface, as done in [55].

A second question concerns the choice of boundary conditions for the volume fraction as well. In the introduction of this paper, we have mentioned that numerical studies employing the no-slip boundary condition have been unsuccessful in reproducing the volume fraction profiles near the wall. This holds for a large class of volume fraction boundary condition: Dirichlet conditions [23, 24], zero-particle flux conditions [6, 10, 11] and symmetry based conditions [7] that produce almost identical results. However, whether this result carries over to the case of apparent slip boundary conditions remains an open question.

A third question concerns the overall extendability of our analysis to other types of flows. To examine this question it is advisable to dichotomize flows into steady unidirectional flows and transient and multidimensional ones in complex geometries. As regards the first category, one could in principle try to derive analytic solutions for different boundary conditions. In turn, this facilitates the exact identification of the differences in the solution profiles.

While the derivation of analytic solution is not alien to granular flow models, it has been confined to dry granular flows [56, 57] or mixture suspension models [58]. Extending the ideas of these works to two-phase models is very unlikely and thus one needs to resort to numerical simulations. In that case the lessons learned from this study would be useful for the development and calibration of the corresponding algorithms.

As regards more complicated flows, e.g. transient and multidimensional ones in complex geometries, there is a trade-off that should be accounted for. It is well known that Eulerian-Eulerian models can be cumbersome to integrate numerically due to the size and complexity of the governing equations, [27]. Accommodating apparent slip boundary conditions, which fall within the category of Robin-type, introduces extra layers of complexity on both the algorithmic and implementation level. Thus, prior to opting away from the classical no-slip condition, one should at least forecast on the benefits such as, for instance, in the overall accuracy of the numerical predictions. This can be exemplified via two case studies. For our first case study, we consider the process of particle erosion from the surface of a subaqueous bed. For such a flow, one could expect that for sufficiently thick beds the lower part of the bed remains at still. Consequently, choosing between an apparent slip and a no-slip boundary condition is going to have little impact on the overall results; indeed, both experimental measurements [59] and Discrete Element Method (DEM) simulations [60] confirm that. For our second case study, consider the problem of the granular column collapse. Experiments and numerical simulations for both the subaerial [28, 61, 62] and the subaqueous [25, 35, 63–66] configuration assert that, independently of the physical properties of the interstitial medium, the travelling front that forms upon the onset of the collapse has non-zero granular velocity up to the bottom surface. Consequently, changes in the boundary conditions will translate into changes in the predicted properties, e.g. final distance of the pile, and thus affect the overall fidelity of the simulations.

References

[1] A. Karnis, H. Goldsmith, S. Mason, The kinetics of flowing dispersions: I. concentrated suspensions of rigid particles, J. Colloid Interf. Sci. 22 (1966) 531 – 553.

[2] C. J. Koh, P. Hookham, L. G. Leal, An experimental investigation of

concentrated suspension flows in a rectangular channel, J. Fluid. Mech. 266 (1994) 1–32.

[3] M. K. Lyon, L. G. Leal, An experimental study of the motion of concentrated suspensions in two-dimensional channel flow. part 1. monodisperse systems, J. Fluid. Mech. 363 (1998) 25–56.

[4] C. Gao, B. Xu, J. F. Gilchrist, Mixing and segregation of microspheres in microchannel flows of mono- and bidispersed suspensions, Phys. Rev. E 79 (2009) 036311.

[5] C. Gao, S. D. Kulkarni, J. F. Morris, J. F. Gilchrist, Direct investigation of anisotropic suspension structure in pressure-driven flow, Phys. Rev. E 81 (2010) 041403.

[6] R. J. Phillips, R. C. Armstrong, R. A. Brown, A. L. Graham, J. R. Abbott, A constitutive equation for concentrated suspensions that accounts for shear-induced particle migration, Phys. Fluids A 4 (1992) 30–40.

[7] D. Monsorno, C. Varsakelis, M. Papalexandris, Poiseuille flow of dense non-colloidal suspensions: The role of intergranular and nonlocal stresses in particle migration, J. Non-Newton. Fluid 247 (2017) 229–238.

[8] M. Massoudi, K. Rajagopal, T. Phuoc, On the fully developed flow of a dense particulate mixture in a pipe, Powder Technol. 104 (1999) 258 – 268.

[9] B. Lecampion, D. I. Garagash, Confined flow of suspensions modelled by a frictional rheology, J. Fluid. Mech. 759 (2014) 197–235.

[10] K. Yapici, R. L. Powell, R. J. Phillips, Particle migration and suspension structure in steady and oscillatory plane poiseuille flow, Phys. Fluids 21 (2009) 053302.

[11] R. M. Miller, J. F. Morris, Normal stress-driven migration and axial development in pressure-driven flow of concentrated suspensions, J. Non-Newton. Fluid 135 (2006) 149 – 165.

[12] Y. Li, J. Fu, Z. Geng, H. Dong, Cfd simulations of shear induced migration in pressure-driven flow with non-brownian suspensions, International Journal of Multiphase Flow 147 (2022) 103918.

[13] R. E. Hampton, A. A. Mammoli, A. L. Graham, N. Tetlow, S. A. Altobelli, Migration of particles undergoing pressure-driven flow in a circular conduit, Journal of Rheology 41 (1997) 621–640.

[14] K. Yeo, M. R. Maxey, Numerical simulations of concentrated suspensions of monodisperse particles in a poiseuille flow, J. Fluid. Mech. 682 (2011) 491–518.

[15] P. R. Nott, J. F. Brady, Pressure-driven flow of suspensions: simulation and theory, J. Fluid. Mech. 275 (1994) 157–199.

[16] T. Dbouk, E. Lemaire, L. Lobry, F. Moukalled, Shear-induced particle migration: Predictions from experimental evaluation of the particle stress tensor, Journal of Non-Newtonian Fluid Mechanics 198 (2013) 78–95.

[17] I. Drijer, T. van de Laar, H. Vollebregt, C. Schroën, From highly specialised to generally available modelling of shear induced particle migration for flow segregation based separation technology, Separation and Purification Technology 192 (2018) 99–109.

[18] M. K. Lyon, L. G. Leal, An experimental study of the motion of concentrated suspensions in two-dimensional channel flow. part 2. bidisperse systems, Journal of Fluid Mechanics 363 (1998) 57–77.

[19] P. Gondret, L. Petit, Dynamic viscosity of macroscopic suspensions of bimodal sized solid spheres, Journal of Rheology 41 (1997) 1261–1274.

[20] M. E. Gurtin, W. O. Williams, An axiomatic foundation for continuum thermodynamics, Archive for Rational Mechanics and Analysis 26 (1967) 83–117.

[21] M. B. Allen, Mechanics of multiphase fluid flows in variably saturated porous media, International Journal of Engineering Science 24 (1986) 339–351.

[22] S. Benyahia, M. Syamlal, T. J. O'Brien, Extension of Hill–Koch–Ladd drag correlation over all ranges of Reynolds number and solids volume fraction, Powder Technol. 162 (2006) 166–174.

[23] Y. Wang, K. Hutter, A constitutive model of multiphase mixtures and its application in shearing flows of saturated solid-fluid mixtures, Granul. Matter 1 (1999) 163–181.

[24] M. A. Goodman, S. C. Cowin, Two problems in the gravity flow of granular materials, J. Fluid. Mech. 45 (1971) 321–339.

[25] D. Monsorno, A. A. Dimas, M. V. Papalexandris, Time-accurate calculation of two-phase granular flows exhibiting compaction, dilatancy and nonlinear rheology, J. Comput. Phys. 372 (2018) 799 – 822.

[26] C. Varsakelis, M. V. Papalexandris, Numerical simulation of subaqueous chute flows of granular materials, Eur. Phys. J. E 38 (2015) 40.

[27] C. Varsakelis, D. Monsorno, M. Papalexandris, Projection methods for two velocity–two pressure models for flows of heterogeneous mixtures, Comput. Math. Appl. 70 (2015) 1024 – 1045.

[28] P.-Y. Lagrée, L. Staron, S. Popinet, The granular column collapse as a continuum: validity of a two-dimensional Navier–Stokes model with a $\mu(I)$-rheology, J. Fluid. Mech. 686 (2011) 378–408.

[29] F. Municchi, P. P. Nagrani, I. C. Christov, A two-fluid model for numerical simulation of shear-dominated suspension flows, International Journal of Multiphase Flow 120 (2019) 103079.

[30] S. C. Jana, B. Kapoor, A. Acrivos, Apparent wall slip velocity coefficients in concentrated suspensions of noncolloidal particles, Journal of Rheology 39 (1995) 1123–1132.

[31] F. Soltani, U. Yilmazer, Slip velocity and slip layer thickness in flow of concentrated suspensions, Journal of Applied Polymer Science 70 (1998) 515–522.

[32] M. Cloitre, R. T. Bonnecaze, A review on wall slip in high solid dispersionsac, Rheol. Acta 56 (2017) 283–305.

[33] P. Wilms, J. Wieringa, T. Blijdenstein, K. van Malssen, J. Hinrichs, R. Kohlus, On the difficulty of determining the apparent wall slip of highly concentrated suspensions in pressure driven flows: The accuracy of indirect methods and best practice, Journal of Non-Newtonian Fluid Mechanics 299 (2022) 104694.

[34] L. Rondon, O. Pouliquen, P. Aussillous, Granular collapse in a fluid: Role of the initial volume fraction, Physics of Fluids 23 (2011) 073301.

[35] C. Wang, Y. Wang, C. Peng, X. Meng, Dilatancy and compaction effects on the submerged granular column collapse, Physics of Fluids 29 (2017) 103307.

[36] C.-H. Lee, Z. Huang, M.-L. Yu, Collapse of submerged granular columns in loose packing: Experiment and two-phase flow simulation, Physics of Fluids 30 (2018) 123307.

[37] A. Gavrilov, A. Shebelev, Single-fluid model of a mixture for laminar flows of highly concentrated suspensions, Fluid Dyn. 53 (2018) 255–269.

[38] D. M. Kalyon, Apparent slip and viscoplasticity of concentrated suspensions, J. Rheol. 49 (2005) 621–640.

[39] D. Monsorno, C. Varsakelis, M. Papalexandris, A two-phase thermomechanical theory for granular suspensions, J. Fluid. Mech. 808 (2016) 410–440.

[40] M. V. Papalexandris, A two-phase model for compressible granular flows based on the theory of irreversible processes, J. Fluid. Mech. 517 (2004) 103–112.

[41] C. Varsakelis, M. V. Papalexandris, Low-Mach-number asymptotics for two-phase flows of granular materials, J. Fluid. Mech. 669 (2011) 472–497.

[42] J. F. Morris, F. Boulay, Curvilinear flows of noncolloidal suspensions: The role of normal stresses, J. Rheol. 43 (1999) 1213–1237.

[43] J. M. Powers, D. S. Stewart, H. Krier, Analysis of Steady Compaction Waves in Porous Materials, J. Appl. Mech. 56 (1989) 15–24.

[44] Y. Lam, Z. Wang, X. Chen, S. Joshi, Wall slip of concentrated suspension melts in capillary flows, Powder Technology 177 (2007) 162–169.

[45] M. Han, C. Kim, M. Kim, S. Lee, Particle migration in tube flow of suspensions, Journal of Rheology 43 (1999) 1157–1174.

[46] M. S. Ingber, A. L. Graham, L. A. Mondy, Z. Fang, An improved constitutive model for concentrated suspensions accounting for shear-induced particle migration rate dependence on particle radius, Int. J. Multiphas. Flow 35 (2009) 270–276.

[47] R. Delannay, M. Louge, P. Richard, N. Taberlet, A. Valance, Towards a theoretical picture of dense granular flows down inclines, Nature Materials 6 (2007) 99–108.

[48] P. V. Dsouza, P. R. Nott, A non-local constitutive model for slow granular flow that incorporates dilatancy, Journal of Fluid Mechanics 888 (2020) R3.

[49] J. M. Hill, D. Bhattacharya, W. Wu, Bagnold velocity profile for steady-state dense granular chute flow with base slip, Rheologica Acta 61 (2022) 207 – 214.

[50] A. D. Rosato, H. Kim, Particle dynamics calculations of wall stresses and slip velocities for couette flow of smooth inelastic spheres, Continuum Mechanics and Thermodynamics 6 (1994) 1–20.

[51] R. Artoni, A. C. Santomaso, M. Go', P. Canu, Scaling laws for the slip velocity in dense granular flows, Phys. Rev. Lett. 108 (2012) 238002.

[52] W. Liu, C.-Y. Wu, Analysis of inertial migration of neutrally buoyant particle suspensions in a planar poiseuille flow with a coupled lattice boltzmann method-discrete element method, Physics of Fluids 31 (2019) 063301.

[53] G. C. Yang, L. Jing, C. Y. Kwok, Y. D. Sobral, Size effects in underwater granular collapses: Experiments and coupled lattice boltzmann and discrete element method simulations, Phys. Rev. Fluids 6 (2021) 114302.

[54] M. W. Richman, Boundary conditions based upon a modified maxwellian velocity distribution for flows of identical, smooth, nearly elastic spheres, Acta Mechanica 75 (1988) 227–240.

[55] R. Artoni, A. Santomaso, P. Canu, Effective boundary conditions for dense granular flows, Phys. Rev. E 79 (2009) 031304.

[56] X. Meng, Y. Wang, F. Feng, C. Wang, Y. Zhou, Granular flows in a rotating drum and on an inclined plane: Analytical and numerical solutions, Physics of Fluids 30 (2018) 106605.

[57] T. Barker, C. Zhu, J. Sun, Exact solutions for steady granular flow in vertical chutes and pipes, Journal of Fluid Mechanics 930 (2022) A21.

[58] R. J. Phillips, R. C. Armstrong, R. A. Brown, A. L. Graham, J. R. Abbott, A constitutive equation for concentrated suspensions that accounts for shear-induced particle migration, Physics of Fluids A: Fluid Dynamics 4 (1992) 30–40.

[59] F. Charru, H. Mouilleron, O. Eiff, Erosion and deposition of particles on a bed sheared by a viscous flow, Journal of Fluid Mechanics 519 (2004) 55–80.

[60] A. Kidanemariam, M. Uhlmann, Direct numerical simulation of pattern formation in subaqueous sediment, Journal of Fluid Mechanics 750 (2014) R2.

[61] F. Ceccato, A. Leonardi, V. Girardi, P. Simonini, M. Pirulli, Numerical and experimental investigation of saturated granular column collapse in air, Soils and Foundations 60 (2020) 683–696.

[62] T. Man, H. E. Huppert, L. Li, S. A. Galindo-Torres, Deposition morphology of granular column collapses, Granular Matter 23 (2021) 59.

[63] C. Wang, Y. Wang, C. Peng, X. Meng, Two-fluid smoothed particle hydrodynamics simulation of submerged granular column collapse, Mechanics Research Communications 79 (2017) 15–23.

[64] G. Pinzon, M. Cabrera, Planar collapse of a submerged granular column, Physics of Fluids 31 (2019) 086603.

[65] M. Rauter, The compressible granular collapse in a fluid as a continuum: validity of a navier–stokes model with $\mu(j)$, $\phi(j)$-rheology, Journal of Fluid Mechanics 915 (2021) A87.

[66] C.-H. Lee, J.-Y. Chen, Multiphase simulations and experiments of subaqueous granular collapse on an inclined plane in densely packed conditions: Effects of particle size and initial concentration, Phys. Rev. Fluids 7 (2022) 044301.